

# Ferrimagnetic ground state of a phenylene polymer with organic radicals

W.Z. Wang<sup>1,a</sup> and K.L. Yao<sup>2</sup>

<sup>1</sup> Department of Physics, Wuhan University, Wuhan 430072, PR China

<sup>2</sup> Department of Physics, Huazhong University of Science and Technology, Wuhan 430074, PR China

Received 15 July 2002

Published online 31 December 2002 – © EDP Sciences, Società Italiana di Fisica, Springer-Verlag 2002

**Abstract.** A ferrimagnetic polymer with *m*-phenylene skeleton as coupling unit is studied with the Hubbard model in the self-consistent mean-field theory. The ferrimagnetic ground state with a total spin  $S = 1$  per unit cell is obtained and originates from the antiferromagnetic correlations between the nearest neighbors. If the on-site electron-electron repulsions at the radical sites and at the phenylene ring sites are different, the gap in energy band structure may disappear and the ferrimagnetic ground state becomes unstable. The charge density and spin density can transfer between the radical sites and the phenylene ring sites due to the competition between the hopping integral and the on-site repulsion at different sites.

**PACS.** 71.27.+a Strongly correlated electron systems; heavy fermions – 71.10.Fd Lattice fermion models (Hubbard model, etc.) – 75.30.Fv Spin-density waves

## 1 Introduction

It is well known that ferromagnetic materials, both natural and man-made, are primarily inorganic systems. However, in the past decades, some organic molecule-based ferromagnetic compounds such as *p*-nitrophenyl nitronyl nitroxide (*p*-NPNN) [1–3], dupeyredioxyl (DTDA) [4–6], and 3-(4-chlorophenyl)-1,5-dimethyl-6-thioxoverdazyl (*p*-CDTV) [7] have been synthesized. Because these materials only consist of light elements such as H, C, N, and O, which do not involve spins of either *d* or *f* electrons in common ferromagnetic materials, the mechanism of ferromagnetism in organic polymers containing only  $\pi$ -electrons is, therefore, considerably challenging [8].

The early theoretical model for ferromagnetism in organic solids was based on the stacking of organic radicals so that in neighboring radicals the atoms with positive and negative spin densities are juxtaposed, thereby leading to incomplete spin cancellation [9,10]. For *p*-NPNN, ferromagnetic interaction is introduced by stable free radicals with localized spin structures [1]. The ferromagnetic behaviors are described using the one-dimensional Heisenberg model [11]. For poly-BIPO[1,4-bis-(2,2,6,6-tetramethyl-4-piperidyl)-butadiin], a simplified zigzag structure consisting of carbon atoms in the main chain and the side radicals was proposed [12]. Both  $\pi$ -electron on the main chain and the unpaired electron on the radicals were assumed to be localized and the ferromagnetism is attributed to the antiferromagnetic correla-

tion between the neighboring spins. In the improved theory,  $\pi$ -electrons and radical electrons can be itinerant and the ferromagnetic ground state was studied in Hartree-Fock approximation [13,14]. In very recent articles [15,16], a polymer with bipartite lozenge lattice is also studied by means of the exact diagonalization, Monte Carlo simulation, and Hartree-Fock approximation and rigorous theorem. A ferrimagnetic long-range ordering is obtained for all these models at half filling.

From recent experimental studies of magnetic interactions [17–22], some well-known organic magnetic molecules with the ferro(antiferro)magnetic ground state contain phenylene-bridged organic polyradicals. Density function study of ferromagnetic interaction has been performed for *m*-phenylene molecules with various organic radical groups at *meta* position [23]. The parallel spin configuration between radical sites are more stabilized than the antiparallel ones. Hence, organic high-spin dendrimers and polymers with the ferromagnetic ground state can be designed by linking various radicals through an *m*-phenylene unit. In order to confirm the possibility of designing this kind of ferromagnetic polymer, in this paper, we will study a simplified organic structure shown in Figure 1 which is based on poly-(para)phenylene substituted at the meta-position by radicals. Generally, each of sites 3 and 6 connects to an atom H, and each of the radical sites 5 and 8 is an atom group such as CH<sub>2</sub>, NH etc. Each site on the phenylene ring has a  $\pi$ -electron which is itinerant in this structure. Each side radical has an unpaired electron. The correlation between  $\pi$  electrons as well as their itineracy will be taken into account by the Hubbard

<sup>a</sup> e-mail: wzwang70@hotmail.com

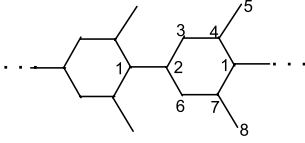


**Fig. 1.** A phenylene polymer with organics radical.

model. The on-site Hubbard repulsion  $U_0$  at the phenylene ring may be quite different from  $U$  at the side radicals. Within mean-field theory, we calculate the spin and charge distribution of the ground state, and obtain the phase diagrams. The results show that in a large range of  $U \neq U_0$ , the spin per unit cell is  $S = 1$  although the charge distribution is not homogeneous. But if  $U$  is much smaller than  $U_0$ , the average spin will reduce in some area of the parameter space. The spin configuration shows that the antiferromagnetic correlation is different for different bonds and results in an unsaturated average spin. In this article, in order to show the basic physics and avoid too many parameters in the discussion, we do not consider other factors such as the possible different on-site energies, the interchain coupling, the next nearest neighboring hopping, inter-site Coulomb interaction, which also results in the transfer of charge density between different sites.

In the following section we define all the parameters of the model Hamiltonian and give the computational method. In Section 3 we study the ground state, the distribution of spin density and charge density. Finally, we summarize our results.

## 2 Model and computational method

The Hamiltonian is written as,

$$H = - \sum_{\langle li, kj \rangle, \sigma} t_{li, kj} (c_{li, \sigma}^\dagger c_{kj, \sigma} + \text{h.c.}) + \frac{1}{2} \sum_{li, \sigma} U_i (n_{li, \sigma} n_{li, -\sigma}), \quad (1)$$

here  $c_{li, \sigma}^\dagger$  ( $c_{li, \sigma}$ ) denotes electron creation (annihilation) operator and  $n_{li, \sigma}$  is electron number operator at site  $i$  in unit cell  $l$  with spin  $\sigma = \alpha, \beta$ .  $\langle li, kj \rangle$  labels the nearest neighbors. We assume the  $\pi$  orbitals on the phenylene ring sites are same and the radical  $\pi$  orbitals are different from those on the phenylene ring. So we have the hopping integral  $t_{li, kj} = t_0$  if  $\langle li, kj \rangle$  connects the phenylene ring sites,  $t_{li, kj} = t$  if  $\langle li, kj \rangle$  connects the phenylene ring site with the radical site. In the following discussion, we take  $t_0$  as energy unit. The Hubbard energy  $U_i$  is equal to  $U_0$  for the phenylene ring site  $i$ , and  $U$  for radical site  $i$ .

We treat the electron-electron interaction in the Hartree-Fock approximation,

$$n_{li, \sigma} n_{li, -\sigma} = \sum_{\sigma} \left( \langle n_{li, -\sigma} \rangle n_{li, \sigma} - \frac{1}{2} \langle n_{li, \sigma} \rangle \langle n_{li, -\sigma} \rangle \right) \quad (2)$$

here,  $\langle \rangle$  is the average with respect to the mean-field-theory ground state. Due to translation symmetry,  $\langle n_{li, \sigma} \rangle = \langle n_{i, \sigma} \rangle$  is independent on  $l$ .

In order to diagonalize the Hamiltonian, we take the Fourier transformation of  $c_{li, \sigma}$ ,

$$c_{li, \sigma} = N^{1/2} \sum_k e^{-ikl} b_{ki, \sigma}, \quad (3)$$

then the Hamiltonian becomes,

$$H = - \sum_{k, \sigma} \mathbf{b}_{k\sigma}^\dagger \mathbf{M}^\sigma(k) \mathbf{b}_{k\sigma} - N \sum_{i=1}^8 U_i \langle n_{i, \alpha} \rangle \langle n_{i, \beta} \rangle. \quad (4)$$

Here,  $\mathbf{b}_{k\sigma}^\dagger$  is an eight-dimensional row vector defined as,

$$\mathbf{b}_{k\sigma}^\dagger = \left( b_{k1, \sigma}^\dagger, b_{k2, \sigma}^\dagger, \dots, b_{k8, \sigma}^\dagger \right) \quad (5)$$

$\mathbf{M}^\sigma(k)$  is a  $8 \times 8$  energy matrix with following nonzero elements:

$$\begin{aligned} M_{i, i+1}^\sigma(k) &= M_{1,4}^\sigma(k) = M_{1,7}^\sigma(k) = M_{2,6}^\sigma(k) = -1, \quad (i = 2, 3, 6) \\ M_{4,5}^\sigma(k) &= M_{7,8}^\sigma(k) = -t, \quad M_{1,2}^\sigma(k) = e^{ik}, \\ M_{j,j}^\sigma(k) &= U_j \langle n_{j, -\sigma} \rangle, \quad (j = 1, 2, \dots, 8), \\ M_{j,i}^\sigma(k) &= (M_{i,j}^\sigma(k))^* \quad (i \neq j). \end{aligned} \quad (6)$$

From the equation

$$\mathbf{M}^\sigma(k) \mathbf{V}_{i\sigma}(k) = E_{i, \sigma}(k) \mathbf{V}_{i\sigma}(k) \quad (i = 1, 2, \dots, 8) \quad (7)$$

we can get an eigenvalue  $E_{i, \sigma}(k)$  and an eigenvector  $\mathbf{V}_{i\sigma}(k)$  of the matrix  $\mathbf{M}^\sigma(k)$ , where  $i$  ( $=1, 2, \dots, 8$ ) is the energy-band index. The unitary transformation  $\mathbf{P}^\sigma(k)$  that diagonalizes  $\mathbf{M}^\sigma(k)$  is given by

$$\mathbf{P}^\sigma(k) = (\mathbf{V}_{1\sigma}(k), \mathbf{V}_{2\sigma}(k), \dots, \mathbf{V}_{8\sigma}(k)). \quad (8)$$

So we can define an eight-dimensional new operator  $\mathbf{a}_{k\sigma}^\dagger = \mathbf{b}_{k\sigma}^\dagger \mathbf{P}^\sigma(k)$  to diagonalize the Hamiltonian equation (4),

$$H = - \sum_{k, \sigma} \sum_{i=1}^8 E_{i, \sigma}(k) a_{ki, \sigma}^\dagger a_{ki, \sigma} - N \sum_{i=1}^8 U_i \langle n_{i, \alpha} \rangle \langle n_{i, \beta} \rangle, \quad (9)$$

here,  $a_{ki, \sigma}^\dagger$  is the  $i$ th component of  $\mathbf{a}_{k, \sigma}^\dagger$ . The ground state can now be written as

$$|G\rangle = \prod_{ki, \sigma}^{(occ)} a_{ki, \sigma}^\dagger |0\rangle, \quad (10)$$

here  $|0\rangle$  is electron vacuum state and  $(occ)$  labels the states occupied by electrons. From equation (10), we can get the charge density:

$$\langle n_{j, \sigma} \rangle = N^{-1} \sum_{ki, \sigma}^{(occ)} V_{ji\sigma}(k) V_{ji\sigma}^*(k), \quad (11)$$

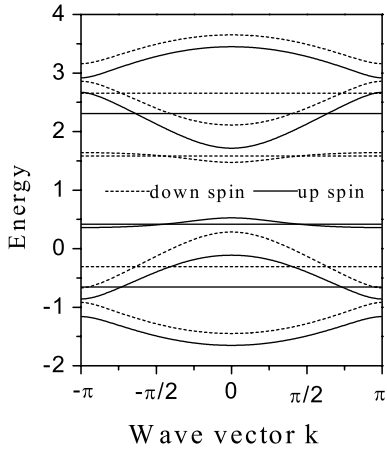


**Fig. 2.** Band spectra for  $t = 1.0$  and  $U = U_0 = 2$ .

here  $V_{ji\sigma}(k)$  is the  $j$ th component of the eigenvector  $\mathbf{V}_{i\sigma}(k)$ .

Because the matrix  $\mathbf{M}^\sigma(k)$  contains the term  $\langle n_{j,\sigma} \rangle$ , we must solve equations (7) and (11) self-consistently. In the following section we will discuss the distributions of the spin density  $\langle S_j^z \rangle$  and the charge density  $\langle n_i \rangle$  which are defined as,

$$\begin{aligned} \langle S_j^z \rangle &= \frac{1}{2}(\langle n_{j,\alpha} \rangle - \langle n_{j,\beta} \rangle), \\ \langle n_j \rangle &= \langle n_{j,\alpha} \rangle + \langle n_{j,\beta} \rangle. \end{aligned} \quad (12)$$

### 3 Results and discussion

In this paper, we consider the half-filling case for the  $m$ -phenylene organic chain shown in Figure 1. We solve equations (7) and (11) self-consistently and get the band structure shown in Figure 2 for  $t = 1.0$  and  $U = U_0 = 2.0$  in unit of hopping integral  $t_0$ . We can see that the spin degeneracy has been lifted due to the Hubbard electron-electron repulsion. The electron band spectra contain eight up-spin energy bands and eight down-spin energy bands. In the ground state, the lowest three down-spin bands and five up-spin bands are occupied. The total spin in a unit is  $S=1$ . So the ground state is ferrimagnetic. It is found that the ferrimagnetism is contributed mainly by the electrons in the two up-spin bands just below the mid gap. Calculation of wave functions shows that these two bands are highly localized and mainly occupied by the electrons at sites 1, 3, 5, 6, 8 in Figure 1.

The distribution of spin density  $\langle S_j^z \rangle$  at eight sites in a unit cell is shown in Figure 3 for  $t = 1.0$  and different Hubbard energy  $U = U_0$ . There is no net spin at sites 2, 4 and 7 when the Hubbard energy is very small. With increasing  $U$ , down spins appear at these sites while up spins at sites 1, 3, 5, 6, 8 increase. There exist antiferromagnetic correlations between nearest neighbors, which are enhanced by the Hubbard electron-electron repulsion. From Figure 3, we also find the spins at sites 2, 4 and 7 are nearly same due to the similar or same topologic environment with three nearest neighbors. The radical sites 5

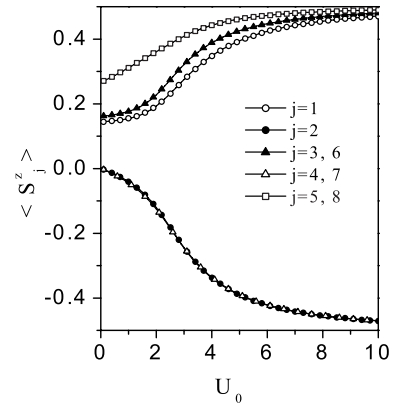


**Fig. 3.** Spin density  $\langle S_j^z \rangle$  at eight sites in a unit cell as a function of the on site repulsion  $U = U_0$  for  $t = 1$ .

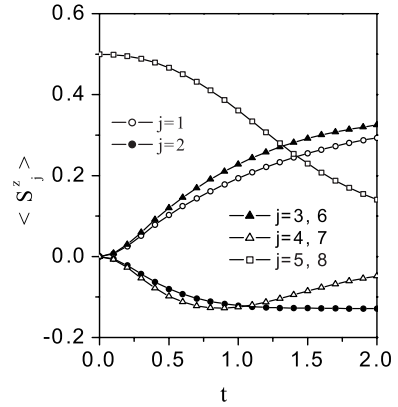


**Fig. 4.** Spin density  $\langle S_j^z \rangle$  at eight sites in a unit cell as a function of the hopping integral  $t$  for  $U = U_0 = 2$ .

and 8 contribute more to the ferrimagnetism. As the interaction  $U$  is large ( $> 10$ ) the spins at different sites approach to their saturations.

When the hopping integral  $t$  between the phenylene ring site and the radical site is different from that between the phenylene ring sites  $t_0$ , the spin density is shown in Figure 4 for  $U = U_0 = 2.0$ . For very small  $t$ , there is no spin at the phenylene ring and the ferrimagnetism is totally contributed by the radical sites. The electrons at radical sites can be considered as parallel local spins. As  $t$  increases, there appears down spin at sites 2, 4, and 7, and up spin at sites 1, 3, and 6. The spins at radical sites decreases with increasing  $t$ . It is seen that due to the difference between  $t$  and  $t_0$ , the behaviors of spin density at site 2 and sites 4, 7 are different (comparing with Fig. 3).

From the band structure, it is found that due to the gap in the middle of the band spectra, the ferrimagnetism results from the difference between the numbers of electrons with up spin and down spin. The greater the gap, more stable the ferrimagnetic ground state. When the on-site repulsion  $U$  at the radical sites is different from  $U_0$  at the phenylene ring sites, the gap may decrease and even disappear. The phase diagram in Figure 5 shows that the gap vanishes below each curve for different  $t$ . When  $U$  is much smaller than  $U_0$ , the gap disappears and the total

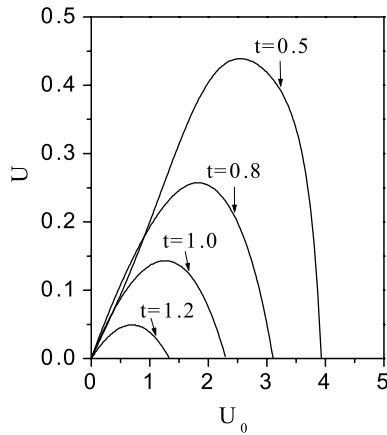


**Fig. 5.** The phase diagram shows the gap disappears below each curve for different  $t$ .

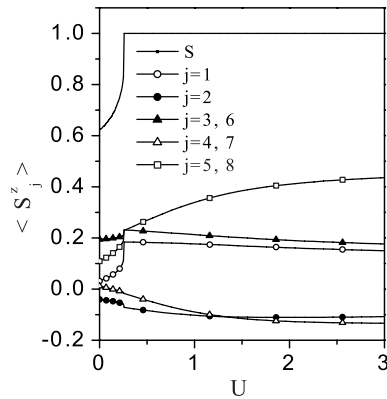


**Fig. 6.** Spin density  $\langle S_j^z \rangle$  as a function of the on site repulsion  $U$  for  $U_0 = 2.0$  and  $t = 0.8$ . The top curve is total spin  $S$ .

spin decreases because the number of electrons with down spin increases. As the radical hopping integral  $t$  decreases, the range of the parameters  $U$  and  $U_0$  to fill the gap becomes wider. For a fairly wider range of the parameters, the gap exists and the ferrimagnetic ground state is stable.

Figure 6 shows the spin density  $\langle S_j^z \rangle$  at each site and the total spin  $S$  as functions of  $U$  for  $U_0 = 2$  and  $t = 0.8$ . As  $U$  is small, the spin density and the antiferromagnetic correlation are small. The gap is filled and the total spin  $S$  in a unit is much smaller than the saturation value  $S = 1$ . As  $U > 0.5$ , the total spin reaches its saturation  $S = 1$  and the antiferromagnetic correlation is enhanced. Especially, the spin density at radical sites get a large increase because the probability with single occupancy is enhanced by the on-site Hubbard energy  $U$ .

When the on-site interaction  $U$  is different from  $U_0$ , the charge density  $\langle n_j \rangle$  is not distributed homogeneously. Figure 7 shows the charge density as a function of  $U$  for  $U_0 = 2.0$  and  $t = 1$ . As  $U$  is small, the charge density moves to the radical sites due to the large on-site repulsion  $U_0$  at phenylene ring sites. When  $U$  increases to about 0.5, there are abrupt changes of charge densities due to the opening of the gap. The continuous increases of  $U$  will enable the charge density to transfer from the radical sites to the phenylene ring. Comparing Figure 7

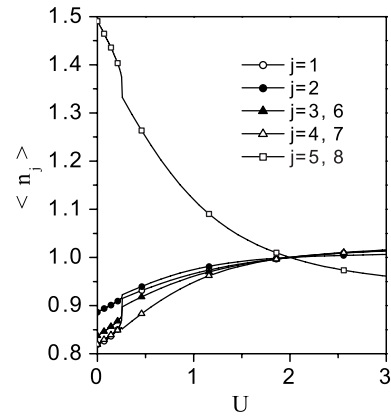


**Fig. 7.** Charge density  $\langle n_j \rangle$  as a function of the on site repulsion  $U$  for  $U_0 = 2.0$  and  $t = 1$ .

with 6, we find that the on-site  $U$  transfers the down-spin electrons to the phenylene ring from the radical sites. If  $U > U_0$ , the charge density at radical sites is greater than that at the phenylene ring sites; if  $U < U_0$ , the behavior is reverse.

In summary, we have studied the ferrimagnetic properties of a *m*-phenylene molecule chain with the Hubbard model in the mean-field theory. The ferrimagnetic ground state with a total spin  $S = 1$  in a unit cell results from the antiferromagnetic correlations between the nearest neighbors. If the on-site electron-electron repulsions at radical sites and the phenylene ring sites are different, the gap in the middle of band spectra may disappear and the ferrimagnetic ground state becomes unstable. The charge density and spin density can transfer between the radical sites and the phenylene ring sites due to the competition between the hopping integral and the on-site repulsion at different sites. It is noticeable that in this paper we just present a probability of ferrimagnetic order at absolute zero temperature. The quantum fluctuation and the thermal excitation of magnon will impact the ferromagnetic order. The interchain interaction in polymer should be also included in future work.

This work is supported by the National Science Foundation of China under the Grant No. 10004004, and the Foundation of Ministry of Education of China under the Grant No. 200034.

## References

1. M. Takahashi, P. Turek, Y. Nakazawa, M. Tamura, K. Nozawa, D. Shiomi, M. Ishikawa, M. Kinoshita, *Phys. Rev. Lett.* **67**, 746 (1991)
2. M. Kinoshita, *Mol. Cryst. Liq. Cryst.* **231**, 1 (1993)
3. M. Tamura, Y. Nakazawa, D. Shiomi, K. Kozawa, Y. Hosokoshi, M. Ishikawa, M. Takahashi, M. Kinoshita, *Chem. Phys. Lett.* **186**, 401 (1991)
4. R. Chiarelli, M.A. Novak, A. Rassat, J.L. Tholence, *Nature* **363**, 147 (1993)
5. R. Chiarelli, A. Rassat, P. Rey, *J. Chem. Soc. Chem. Commun.* **15**, 1081 (1992)

6. R. Chiarelli, A. Rassat, Y. Dromzee, Y. Jeannin, M.A. Novak, J.L. Tholence, *Physica Scripta T* **49**, 706 (1993)
7. K. Mukai, K. Nedachi, J.B. Tamali, N. Achiwa, *Chem. Phys. Lett.* **214**, 559 (1993)
8. J.A. Crayston, J.N. Devine, J.C. Walton, *Tetrahedron* **56**, 7829 (2000)
9. H.M. McConnell, *J. Chem. Phys.* **39**, 1910 (1963)
10. A. Izuoka, S. Murata, T. Sugawara, H. Iwamura, *J. Am. Chem. Soc.* **107**, 1786 (1985)
11. Y. Teki, K. Itoh, A. Okada, H. Yamakage, T. Kobayashi, K. Amaya, S. Kurokawa, S. Ueno, Y. Miura, *Chem. Phys. Lett.* **270**, 573 (1997)
12. Y.V. Korshak, T.V. Medvedeva, A.A. Ovchinnikov, V.N. Spector, *Nature (London)* **326**, 370 (1987); A.A. Ovchinnikov, V.N. Spector, *Synth. Met.* **27**, B615 (1988)
13. Z. Fang, Z.L. Liu, K.L. Yao, *Phys. Rev. B* **49**, 3916 (1994)
14. W.Z. Wang, Z.L. Liu, K.L. Yao, *Phys. Rev. B* **55**, 12989 (1997)
15. A.M.S. Macedo, M.C. dos Santos, M.D. Coutinho-Filho, C.A. Macedo, *Phys. Rev. Lett.* **74**, 1851 (1995)
16. Guang-Shan Tian, Tsung-Hang Lin, *Phys. Rev. B* **53**, 8196 (1996)
17. A. Rajca, J. Wongsriratanakul, S. Rajca, *J. Am. Chem. Soc.* **119**, 11674 (1997)
18. Y.J. Pu, M. Takahashi, E. Tsuchida, H. Nishide, *Mol. Cryst. Liq. Cryst.* **334**, 1 (1999)
19. H. Nishide, M. Miyasaka, E. Tsuchida, *J. Orga. Chem.* **63**, 7399 (1998)
20. A. Rajca, S. Rajca, J. Wongsriratanakul, *J. Am. Chem. Soc.* **121**, 6308 (1999)
21. H. Nishide, T. Ozawa, M. Miyasaka, E. Tsuchida, *J. Am. Chem. Soc.* **123**, 5942 (2001)
22. M.P. Struijk, R.A.J. Janssen, *Synth. Metals*, **103**, 2287 (1999)
23. M. Mita, H. Mori, Y. Takano, D. Yamaki, Y. Yoshika, K. Yamaguchi, *J. Chem. Phys.* **113**, 4035 (2000)